Computational Modeling of Magnetic Field Optical Fiber Sensor Considering Temperature Effects

Allamys A. Dias da Silva [1] (ID), Hebio J. B. Oliveira [1] (ID), Henrique P. Alves [2] (ID),
Jehan Fonsêca do Nascimento [3] (ID) , Joaquim F. Martins-Filho [1] (ID)

[1] *Department of Electronics and Systems, Federal University of Pernambuco, Recife, Brazil*
allamys.allan@ufpe.br, hebio.junior@ufpe.br, joaquim.martins@ufpe.br
[2] *Academic Unit of Belo Jardim, Federal Rural University of Pernambuco, Belo Jardim, Brazil*
henrique.patriota@ufrpe.br
[3] *Interdisciplinary Nucleus for Exact and Natural Sciences, Federal University of Pernambuco,
Caruaru, Brazil*
jehan.nascimento@ufpe.br

Abstract— **Due to the vast area of application and reliability, fiber optic magnetic field sensors have been the subject of several studies, however, some of these application areas are submitted to temperature variations, which can hinder the sensors in monitoring the magnetic field. With this panorama, this work analyzes through computational modeling a fiber optical magnetic field sensor, using the magneto-optical Faraday effect and observing temperature effects in the sensor response. For modeling, a numerical model built in COMSOL Multiphysics is used. The results show a value for cross-sensitivity of 3.27 mT/°C in a non-optimized configuration of the sensor and of 2.47 mT/°C for an optimized configuration. A methodology for optimizing the sensor to operate in a certain temperature range, 55 to 75 °C, is also discussed. The results presented in this work show that the temperature is an important factor to be considered to improve the selectivity and to obtain the correct sensitivity of the sensor.**

Index Terms— **COMSOL, magnetic field sensor, magneto-optical Faraday effect, temperature compensation.**

I. INTRODUCTION

Currently, the sensing of the magnetic field is of great importance in the most diverse areas, some of its applications being: navigation, data storage, geophysics, space systems, medical/biological diagnostics, control and monitoring of industrial processes [1], [2]. Monitoring techniques that use optical fiber sensor offer several advantages such as simplicity, versatility, safety, low weight and reliability [3]. Furthermore, they can carry optical signals over long distances without appreciable loss of power and are free from external electromagnetic interference [4]. The most used detection techniques by optical fiber magnetic field sensors use modal interferometry, Fabry-Perot cavity, Bragg gratings and magneto-optical effects [5]-[9].

The magnetic field produced by electrical equipment can be an important indicator of its proper functioning. As, for example, in a power transformer used in an electric power transmission line, where most of the problems are caused by faults in the transformer winding and terminals, and these

faults can be detected through the variation of the magnetic flux generated by the transformer [10]. In the literature, there are proposals for non-optical sensors aimed at monitoring the nominal magnetic field of transformers in operation [10], as well as sensors that detect the residual magnetic field in transformers not in operation [11]. A possible technological application of fiber optics magnetic field sensors proposed in this manuscript is the monitoring of the nominal magnetic field in transformers, where, in addition to possible changes in the magnetic field, there are also temperature variations [12].

Some studies of magnetic field sensors, found in the literature, point out the importance of temperature compensation in the sensor response [5]-[8]. Some studies show that variations from 1ºC are already sufficient to interfere with the correct monitoring of the magnetic field, making it necessary to compensate for the temperature variation [5], [6]. A proposed solution is to use two sensor heads, one to monitor the temperature, so that it is possible to calibrate the sensor according to temperature, as an example a Bragg grid fiber can be used [7], [8]. Another sensor proposal is based on modal interference and uses the fact that different modes have different sensitivities to the magnetic field parameters and temperature. Thus, by monitoring the signals of different mode orders, it is possible to relate the sensitivities in order to obtain magnetic field and temperature data simultaneously [9].

In this paper, a study of the influence of temperature on the fiber optic magnetic field sensor proposed in a previous work is shown [12]. It is a sensor based on magneto-optical Kerr and Faraday effects, which use iron and Ce:YIG as sensitive media. The manuscript focuses on the results for the structure of the sensor that uses Ce:YIG, since iron has its magnetic response little altered in the temperature range studied here, 25-75 ºC, [14], [15]. The proposed sensor is reflectometric and has high sensitivity with a wide operating range compared to sensors described in the literature [5]-[9]. Computational modeling uses the Finite Element Method, through COMSOL Multiphysics.

Section II presents a description of the Faraday magneto-optical effects, while the computational modeling is presented in Section III. The results and discussions obtained by the study carried out in this work are presented in Section IV. Section V brings the conclusions of the article.

II. MAGNETO-OPTICAL EFFECT

In general, the magneto-optical effect describes the interaction of light with magnetized matter [16]. This effect is observed by the birefringence generated in the magnetic material by the external magnetic field. The magneto-optical response of the material is described by the relative electrical permittivity tensor of the magnetic material as [16]

$$\boldsymbol{\varepsilon} = \varepsilon \begin{pmatrix} 1 & jm_zQ_0 & -jm_yQ_0 \\ -jm_zQ_0 & 1 & jm_xQ_0 \\ jm_yQ_0 & -jm_xQ_0 & 1 \end{pmatrix}, \tag{1}$$

where ε is the relative permittivity of the unmagnetized magnetic material, Q_0 is the magneto-optical constant and $\vec{m} = (m_x, m_y, m_z)$ is the normalized magnetization of the material. At optical frequencies the relative permeability is approximately 1.

Using (1) in Maxwell's equations, two normal modes of propagation in the magnetized material are obtained, which are circular polarizations with refractive indices

$$N_\pm = N\left(1 \pm \frac{1}{2}Q_0\vec{m}.\vec{e}_k\right), \tag{2}$$

being the (+) index for circular polarization on the right and the (-) on the left, $\vec{e}_k$ the propagation direction of light and N the refractive index of the non-magnetized material [16].

The magneto-optical Faraday effect is observed by rotating the polarization of the optical signal transmitted in a magnetic material. Expression (3) describes the Faraday rotation angle, obtained for a wave that passes through a material in the same direction as the magnetic field [17]

$$\phi_B = \frac{\pi d N Q_0 m_x}{\lambda}, \tag{3}$$

where λ is the wavelength of light in a vacuum and d is the thickness of the magnetic material. It is important to highlight that, in the Faraday effect, the wave propagation direction does not change the effect. Therefore, an EM wave traveling around the material of thickness d has a Faraday rotation angle of $2\phi_B$.

Considering a material magnetized in only one direction, e_x, the refractive index expressed in (2) for the magnetized material is given by

$$N_\pm = N\left(1 \pm \frac{1}{2}Q_0 m_x\right). \tag{4}$$

Being the saturation value for the normalized magnetization $m_x = 1$ and the complex refractive index of the magnetic material described by $N = n + j\kappa$, where n is the real part of the refractive index and κ is the extinction coefficient, we have that the magneto-optical constant of the magnetic material is given by

$$Q_0 = \frac{\lambda\phi_B^{\max}}{\pi d}\frac{n}{n^2 + \kappa^2} - j\frac{\lambda\phi_B^{\max}}{\pi d}\frac{\kappa}{n^2 + \kappa^2} = Q_0^{'} - jQ_0^{"} \ . \tag{5}$$

III. COMPUTATIONAL MODELING

This section describes the computational modeling for magnetic field sensor profiling to fiber optics. Fig. 1 shows the architecture of the sensor system for magnetic field detection using magneto-optical effect. Through the figure, it is possible to understand the functioning of the sensor, which consists of a laser, coupled to an optical fiber, emitting an optical signal with a wavelength of 1550 nm. This signal passes through the region of the optical fiber, where the polarization controller (PC) with respect to the direction of polarization P toward the direction of polarization S. Then, the polarized signal passes through port 1 of the optical circulator (OC), leaving port 2, and goes to the

transducer, where the signal is modulated, according to the magnetic field, and reflected towards the OC. After entering port 2 and exiting port 3 of the circulator, the light passes through a polarizing fiber (PF), and it has part of its intensity filtered according to the modulation suffered by the transducer. Finally, the part of the light that passes through the PF is detected by a power detector.
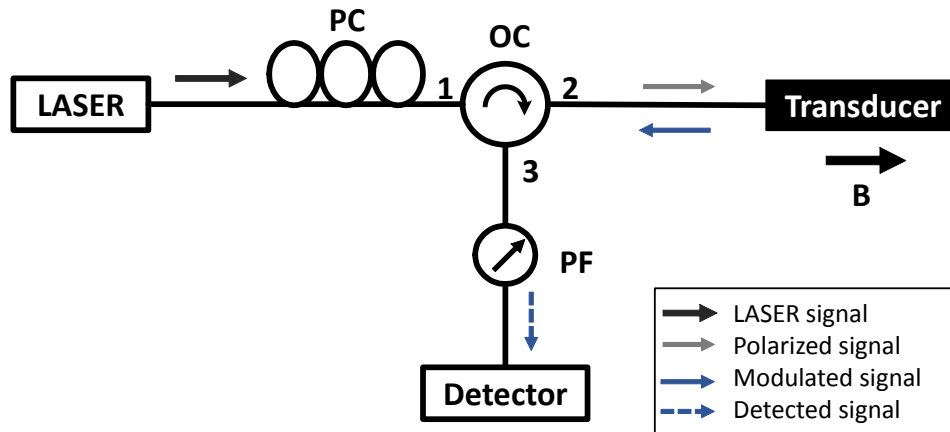

Fig. 1. Fiber optic sensor system architecture for magnetic field monitoring using magneto-optical effect. The system is all in optical fiber and is composed of a LASER at 1550 nm, a polarization controller (PC), an optical circulator (OC), the transducer (modeled in this paper), a polarizing fiber (PF) and a power detector.

The numerical model for the optical fiber magnetic field sensor is implemented in COMSOL Multiphyics, which is a computational modeling software based on the Finite Element Method (FEM) [18]. This software allows the simulation of the transducer element, considering the 2D geometry of an optical fiber, as shown in Fig. 2.
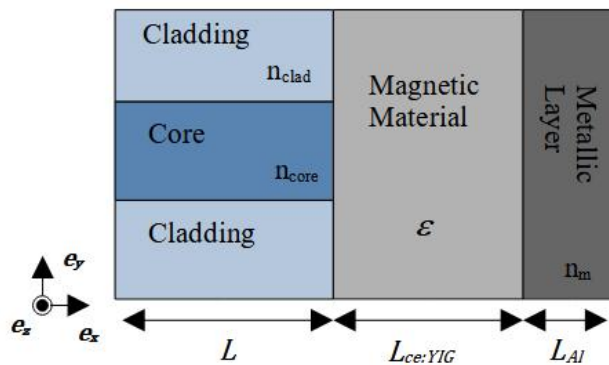

Fig. 2. Fiber optic magnetic field sensor transducer element.

Fig. 2 shows the 2D geometry, which represents the longitudinal section of a single-mode optical fiber, with a magnetic material composed of Ce:YIG, as a transducer element, and a thick layer of metallic material composed of aluminum, to generate signal reflection back to the fiber. It is important to highlight that, in computational modeling, the magneto-optical effect is introduced only using the relative electrical permittivity tensor, expressed in (1). This allows the simulation to resemble a real experiment, while an analytical model has approximations. The excitation of the electromagnetic wave in the structure is done in the form of a Gaussian beam, which is a good approximation for the

fundamental mode that propagates in a single-mode fiber [19]. And the reflectances for the S and P waves are defined in terms of the electric field collected at the left end of the model represented in Fig. 2, which is the initial interface of the optical fiber, according to the following expressions

$$R_s = \frac{\int \left\| E_z - E_z^{in} \right\|^2 dz}{\int \left\| E^{in} \right\|^2 dz} \; ; \quad R_p = \frac{\int \left\| E_y - E_y^{in} \right\|^2 dy}{\int \left\| E^{in} \right\|^2 dy} \; . \tag{6}$$

where E_z^{in} and E_y^{in} are the components of the electric field initially excited in the fiber, E_{in}, while E_z and E_y are the components of the total electric field at the initial interface of the optical fiber.

The values of the parameters used to characterize the materials in the modeling are in the Table I.

TABLE I. PARAMETERS USED IN NUMERICAL SIMULATION

Description	Parameter	Value
Wavelength	λ	1550 nm
Fiber optic core refractive index at 1550 nm [20]	n_{core}	1.444
Fiber optic cladding refractive index at 1550 nm [20]	n_{clad}	1.4378
Ce:YIG Refractive index at 1550 nm [21]	N_m	$2.25+j8.3\times10^{-5}$
Al refraction index at 1550 nm [22]	n_m	$1.5137+j15.234$
Ce:YIG magneto-optical constant	$Q_0^{Ce:YIG}$	$-2.41\times10^{-2}+j8.9\times10^{-7}$
Optical fiber length	L	3 μm
Al layer thickness	L_{Al}	1 μm
Optical fiber Core Diameter	D_{core}	8 μm
Optical fiber cladding diameter	D_{clad}	20 μm

IV. RESULTS AND DISCUSSIONS

Due to the sensor structure, in addition to the Faraday effect, there is a cavity effect (etalon), which influences the signal modulation. Thus, to optimize the sensor sensitivity, a specific combination of the polarization angle of the input optical signal and the thickness of the magnetic material is needed. Following the procedure described in [13], a simulation study can be performed to optimize the structure to operate in the range of 0 to 0.2 T, Ce:YIG saturation field [21], and the configuration with 10° polarization of the input optical signal and 4.3 μm thickness of Ce:YIG is selected. This region is selected because it has high sensitivity, approximately constant throughout the operating range.

The optimization procedure and results presented in [13] were generated considering that the transducer is at room temperature (25 °C). However, there are situations in which the sensor can be under considerable temperature variations throughout the day, such as, for example, inside a power transformer [12]. Therefore, it is necessary to know how temperature affects the modulation of the optical signal.

The effect of temperature can be included in the model through the rate of change of the refractive index of each material in relation to temperature, *dn/dT,* and the change in the magneto-optical constant of Ce:YIG, which can be calculated using the rate of change of the Faraday rotation of Ce:YIG in relation to temperature, *dϕB/dT*. For the Faraday rotation of Ce:YIG we have the rate *dϕB/dT* = 13°/cm/°C [23], and for the refractive indices of materials *dn/dT* = 10^{-5}, 2.5×10^{-4} and 10^{-3} °C^{-1}, respectively for SiO_2 , Ce:YIG and Al [22], [23]. The thermal expansion effect of the magnetic material was neglected, since it has a very small contribution to the signal modulation compared to the other thermal effects considered, for the conditions addressed in this study. The effects of temperature on the signal are shown in Fig. 3, where the S-wave reflectance curve for the fiber optic model is observed. The results presented in the figure show that the magneto-optical response is much more sensitive to temperature than the purely optical response due to the variation of the material's refractive index with temperature. That is, the polarization angle and thickness setting of Ce:YIG that was chosen falls in a region of stability of the etalon effect in the sensor structure, thus, the small change in the refractive index produces a negligible change in the reflectance level of the signal.
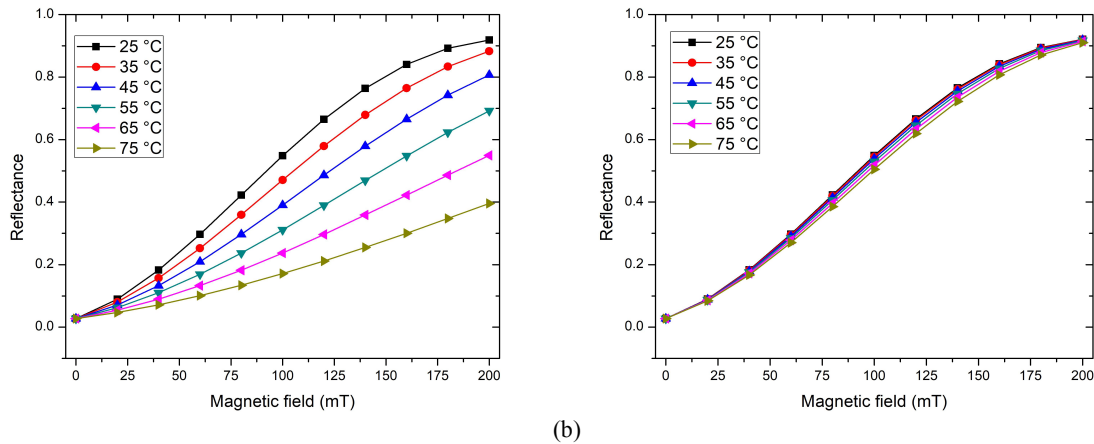

Fig. 3. Reflectance curves for S-wave considering (a) the effect of temperature on the magneto-optical response and the refractive index, and (b) considering only the effect of temperature on the refractive index response (without considering

Once the sensor thickness is determined, reflectance becomes a function of the temperature and the field, *R(B,T)*, so using the results in Fig. 3 (a), it is possible to measure the sensitivity to variations in the field and temperature of the system, being the sensitivity to the magnetic field

$$S_B = \frac{R(B_{sat},T) - R_0}{B_{sat}},$$ (7)

and sensitivity to the temperature,

$$S_T = \frac{R(B,T_2) - R(B,T_1)}{T_2 - T_1},$$ (8)

where T_1 and T_2 are two temperature values that define a range. Thus, the sensitivity to the magnetic field varies with the temperature of the sensing region, as well as the sensitivity to temperature varies with the magnetic field over the region. These sensitivity behaviors are illustrated in Fig. 4, considering the temperature range of 25 – 75 °C.
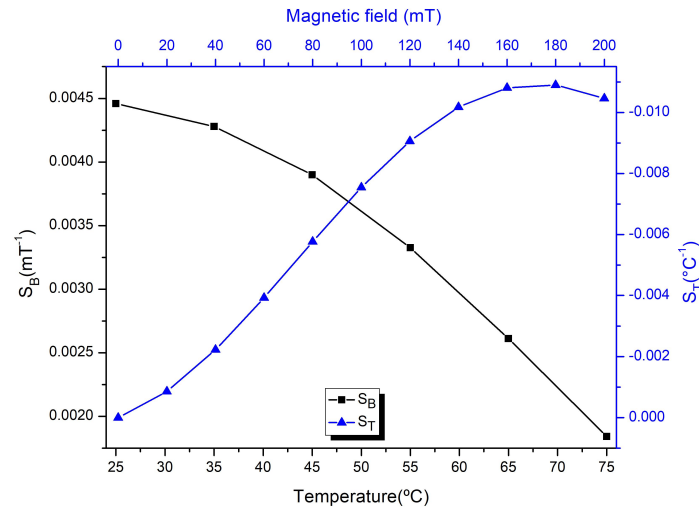

Fig. 4. Sensitivities with respect to the magnetic field as a function of temperature in the sensing region, curve and axes in black, and to temperature as a function of the magnetic field in the sensing region, curve and axes in blue.

According to Fig. 4, a 45% drop in S_B is observed when the operating temperature of the sensor is 50 °C higher in relation to the ambient temperature (25 °C), which shows a marked decrease in sensitivity to magnetic field when temperature increases. Also in Fig. 4, the behavior of the S_T is observed, in which, from 70 mT, it shows that the signal modulation is more sensitive to temperature variations of the order of 1 °C than to variations of 1 mT in the field , since for fields above 70 mT, S_T has a module value higher than 0.0045 °C^{-1}, while S_B has a maximum value of 0.00446 mT^{-1}.

The analysis of how temperature interferes with the field measurement can be done through the relationship between the S_B and S_T sensitivity, for example, if the sensor is operating at room temperature (55 °C), and under the action of a 160 mT magnetic field, the ratio S_T over S_B gives a value of 3.27 mT/°C, which means that a 10°C increase in temperature would cause a variation of 32.7 mT in the field measurement.

Taking into account the application of magnetic field measurement in environments with high temperatures and temperature variations, such as in power transformers, it is necessary to design the sensor in order to optimize the signal for these conditions. This can be done through an analysis observing the behavior of ΔR with respect to temperature and the thickness of the Ce:YIG film. The result is in the surface plot of Fig. 5, for a temperature range of 55 to 75 °C. The purpose of this graph is to allow the choice of a thickness for the Ce:YIG film that provides a high reflectance variation with the magnetic field, and a minimum variation with the temperature. As illustrated in the Fig. 5, this thickness was 8.68 μm.
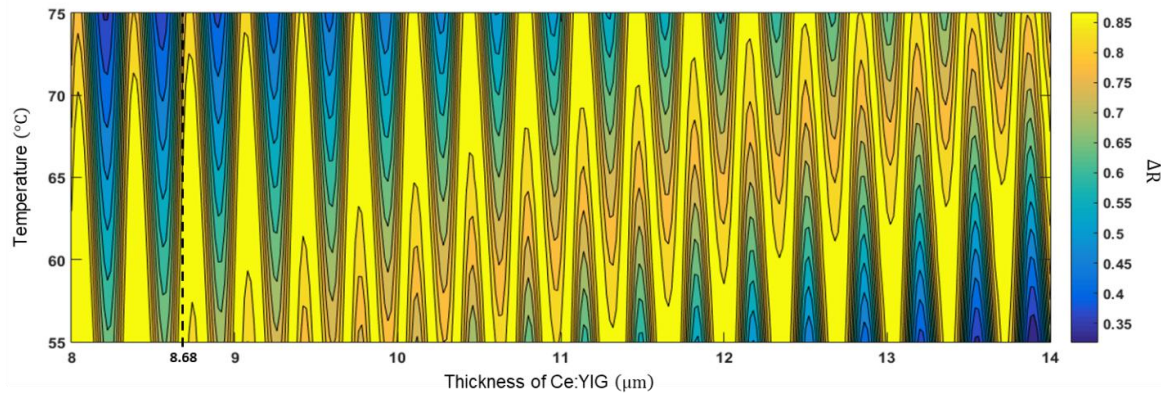
Fig. 5. ΔR level curves for a variation from a null magnetic field to the Ce:YIG saturation field.

Then, with this new structure for the transducer, with the incident wave polarization being 10° and the Ce:YIG thickness 8.68 μm, the results of Fig. 6a were generated, which shows the reflectance of the S wave as a function of the field for temperatures in the range 55-75 °C. To analyze the effect of etalon in this temperature range, the Fig. 6b was generated, where the dependence of the refractive index of materials with temperature was not considered. Comparing the graphs in Fig. 6, it is observed that the one that considers the change in refractive indices with temperature has its curves closer to each other, as well as having larger reflectance variations. Therefore, the etalon effect can be combined with the magneto-optical effect, in order to obtain a better result for the signal modulation.
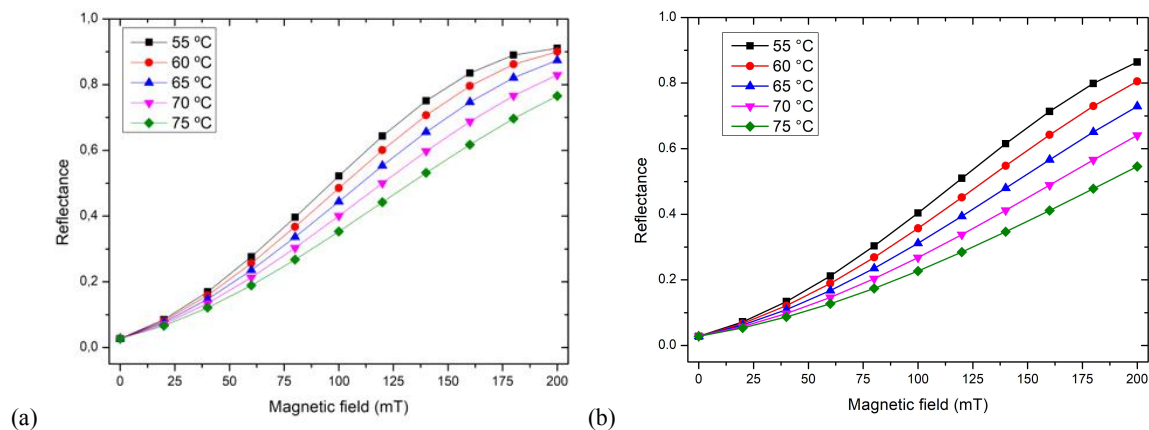

Fig. 6. Reflectance curves for S-wave considering (a) the effect of temperature on the magneto-optical response and the refractive index, and (b) considering only the effect of temperature on the magneto-optical response (without considering the effect on the refractive index).

Using the results of Fig. 6 (a), the sensitivities to field and temperature are calculated according to (7) and (8), which are shown in Fig. 7. Comparing these sensitivity results with those of Fig. 4, it should be noted that sensitivity to the temperature does not change considerably. However, sensitivity to the field is increased by 32.43% for a temperature of 55°C, and up to 100.54% for 75°C. Calculating the cross sensitivity of S_T over S_B, with temperature conditions of 55 °C, and under the action of a 160 mT field, a value of 2.47 mT/°C is obtained.
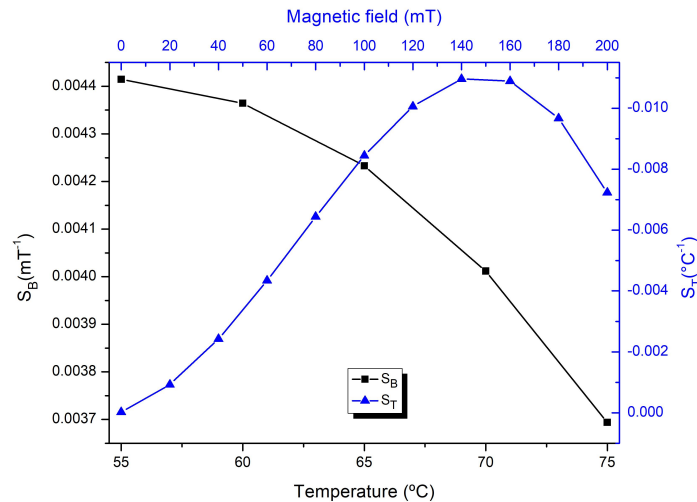
Fig. 7. Sensitivities with respect to the magnetic field as a function of temperature in the sensing region, curve and axes in black, and to temperature as a function of the magnetic field, curve and axes in blue, for an optimized structure to act under 55-75 °C.

From the results presented in this section, it is shown that, depending on the application and the location where the sensor will be used, it is possible to design the transducer in order to optimize the signal for a certain temperature variation range, however, the temperature has an influence on the sensor response that has to be taken into account for a correct measurement of the magnetic field.

V. CONCLUSIONS

We present the computational modeling of a Faraday effect magnetic field sensor based on fiber optics, in which the temperature effect was taken into account. The proposed sensor consists of a magneto-optical material (Ce:YIG) coupled to the cleaved face of an optical fiber. The modeling, carried out using the Finite Element Method, considers the effect of temperature on the variation of the refractive index of materials and on the magneto-optical constant of the magnetic material.

The simulation experiments were carried out for the operating range of fields between 0 and 200 mT and a temperature range from 25 to 75 °C. The results show that the dependence of the magneto-optical constant with temperature has a strong influence on the sensor response, and that this influence can be reduced by tuning the interference effect caused by the etalon formed by the sensor structure. It is worth noting that if the objective is to build a sensor that is more independent to temperature variations, iron can be used as a magnetic material instead of Ce:YIG, as done in a previous study [12]. However, it comes with the cost of a lower sensitivity to the magnetic field [12].

Despite the influence of temperature, the results show that it is possible to design the sensor with Ce:YIG in order to have good sensitivity for a predetermined temperature range, as shown for the range from 55 to 75 °C. For practical applications, a magnetic field-independent temperature sensor, like a fiber Bragg Grating sensor, should be used to obtain the temperature for the accurate measurement of the magnetic field with the proposed sensor. Finally, another possible application for

this sensor is to use it to monitor temperature, optimizing its structure for this purpose. Thus, it could use two sensor heads, one optimized for measuring the magnetic field and the other for measuring temperature, to obtain both parameters simultaneously.

REFERENCES

[1] J. Lenz and S. Edelstein, "Magnetic sensors and their applications," *IEEE Sensors Journal*, vol. 6, no. 3, pp. 631–649, 2006.

[2] Y. N. Zhang, N. Zhu, P. Gao, and Y. Zhao, "Magnetic field sensor based on ring WGM resonator infiltrated with magnetic fluid", *Journal of Magnetism and Magnetic Materials*, vol. 493, pp. 165701, 2020.

[3] J. F. Martins-Filho, E. Fontana, J. Guimarães, D. F. Pizzato, and I. J. Souza Coelho. Fiber-optic-based Corrosion Sensor using OTDR. Presented at 6th annual IEEE Conference on Sensors, pp. 1172–1174, 2007.

[4] J. Haus, "Optical Sensors: Basics and Applications". Ed. Wiley-Vch, 2010.

[5] P. Zu, C. C. Chan, W. S. Lew, L. Hu, Y. Jin, H. F. Liew, L. H. Chen, W. C. Wong and X. Dong, "Temperature-insensitive magnetic field sensor based on nanoparticle magnetic fluid and photonic crystal fiber", *IEEE photonics journal*, vol. 4, no. 2, pp. 491-498, 2012.

[6] F. Chen, Y. Jiang, H. Gao and L. Jiang, "A high-finesse fiber optic Fabry–Perot interferometer based magnetic-field sensor", *Optics and Lasers in Engineering*, Elsevier, vol. 71, pp. 62–65, 2015.

[7] M. Yang, J. Dai, C. Zhou, and D. Jiang, "Optical fiber magnetic field sensors with TbDyFe magnetostrictive thin films as sensing materials," *Optics Express*, vol. 17, no. 23, pp. 20777, 2009.

[8] L. Sun, S. Jiang, and J. R. Marciante, "All-fiber optical magnetic-field sensor based on Faraday rotation in highly terbium-doped fiber," *Optics Express*, vol. 18, no. 6, p. 5407, 2010.

[9] Q. Yu et al., "Temperature compensated magnetic field sensor using magnetic fluid filled exposed core microstructure fiber," *IEEE Transactions on Instrumentation and Measurement*, vol. 71, pp. 1–8, 2022.

[10] F. Haghjoo and H. Mohammadi, "Planar sensors for online detection and region identification of turn-to-turn faults in transformers", *IEEE Sensors Journal*, vol. 17, no. 17, pp. 5450-5459, 2017.

[11] D. Cavallera, V. Oiring, J. L. Coulomb, O. Chadebec, B. Caillault and F. Zgainski, "A new method to evaluate residual flux thanks to leakage flux, application to a transformer", *IEEE Transactions on Magnetics*, vol. 50, no. 2, pp. 1005-1008, 2014.

[12] L. Chen, Z. Zheng, S. Liu, L. Guo, and C.Dun, "Temperature prediction on power transformers and the guide on load dispatch". *IEEE Annual Report Conference on Electrical Insulation and Dielectric Phenomena,* pp. 444-447, 2012.

[13] A. A. D. da Silva, H. P. Alves, F. C. Marcolino, J. F. do Nascimento and J. F. Martins-Filho, "Computational Modeling of Optical Fiber-Based Magnetic Field Sensors Using the Faraday and Kerr Magnetooptic Effects", *IEEE Transactions on Magnetics*, vol. 56, no. 9, pp. 1-9, 2020.

[14] C. Kittel. "Introduction to solid state physics." (1976).

[15] C. D. Graham JR. "Temperature dependence of anisotropy and saturation magnetization in iron and iron-silicon alloys," *Journal of Applied Physics,* vol. 31, no. 5, p. S150-S151, 1960.

[16] J. Zak, E. R. Moog, C. Liu and S. D. Bader, "Universal approach to magneto-optics", *Journal of Magnetism and Magnetic Materials*, vol. 89, no. 1-2, pp. 107-123, 1990.

[17] M. Mansuripur, "The faraday effect", *Optics and Photonics News*, vol. 10, no. 11, pp. 32-36, 1999.

[18] COMSOL MULTIPHYSICS, v. 5.2. www.comsol.com. COMSOL AB, Stockholm, Sweden.

[19] D. Marcuse, "Gaussian approximation of the fundamental modes of graded-index fibers" *JOSA*, vol. 68, no. 1, pp. 103-109, 1978.

[20] A. Mendez and T. F. Morse, Specialty Optical Fibers Handbook. San Francisco, CA, USA: Academic, 2011.

[21] T. Goto, M. C. Onbaşli, C. A. Ross, "Magneto-optical properties of cerium substituted yttrium iron garnet films with reduced thermal budget for monolithic photonic integrated circuits", *Optics Express*, vol. 20, no. 27, pp. 28507-28517, 2012.

[22] A. D. Raki´c, A. B. Djuriˇsi´c, J. M. Elazar, and M. L. Majewski, "Optical properties of metallic films for vertical-cavity optoelectronic devices," *Applied Optics,* vol. 37, no. 22, pp. 5271–5283, 1998.

[23] Y. Shoji, T. Nemoto and T. Mizumoto, "Analysis of temperature dependence of Ce: YIG for athermal waveguide optical isolator", *Technical Digest on ECIO/MOC*, P022. 2014.